Jurnal Teknologi

Full Paper

ADJUSTABLE RESISTANCE FEEDBACK PIECEWISE LINEAR INTERPOLATION PHOTOVOLTAIC EMULATOR

Razman Ayop[a*], Chee Wei Tan[a], Norhafezaidi Mat Saman[b], Mohd Rodhi Sahid[a], Zulkarnain Ahmad Noorden[b]

[a]Faculty of Electrical Engineering, Universiti Teknologi Malaysia, 81310, UTM Johor Bahru, Johor, Malaysia
[b]Institute of High Voltage and High Current (IVAT), Faculty of Electrical Engineering, Universiti Teknologi Malaysia, 81310, UTM Johor Bahru, Johor, Malaysia

Article history
Received
30 November 2023
Received in revised form
3 March 2024
Accepted
3 March 2024
Published Online
20 August 2024

*Corresponding author
razman.ayop@utm.my

Graphical abstract

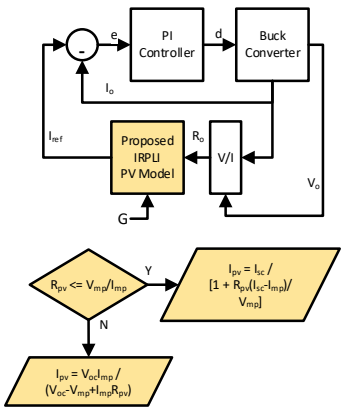

Abstract

Photovoltaic (PV) emulator (PVE) is a power converter that follows the voltage and current characteristic of a PV module. The direct referencing method (DRM) is the prevailing control strategy for the PVE because of its straightforward nature. Nonetheless, stability is an issue for this control strategy. The resistance feedback method (RFM) provides an alternative solution without encountering stability issues. The RFM requires a specialize current-resistance (I-R) PV model to operate. Currently, the adjustable piecewise linear interpolation (PLI) for this specialize PV model is unavailable for the RFM PVE. This paper proposed an adjustable I-R PLI (IRPLI) PV model for the PVE that uses the RFM control strategy. The performance of this PV model and its corresponding RFM PVE is compared with the current-voltage PLI (IVPLI) PV model together with the DRM PVE. The output of the IRPLI is similar to the IVPLI at various irradiance. The discrepancy in error for both PV models is a maximum of 6% when compared to the standard single diode model (SDM) PV model. The IRPLI is 3.2 times faster compared to the SDM and 1.07 times slower compared to the IVPLI. The IRPLI also able to properly integrated with the RFM PVM without any stability issues.

Keywords: Photovoltaic model, piecewise linear interpolation, linear regression, buck converter, PI controller

Abstrak

Pelagak Fotovoltaik (PV) (PVE) merupakan penukar kuasa yang mengikut sifat voltan dan arus modul PV. Kaedah rujukan langsung (DRM) adalah strategi kawalan utama bagi PVE kerana sifatnya yang mudah. Walau bagaimanapun, kestabilan merupakan isu untuk strategi kawalan ini. Kaedah maklum balas rintangan (RFM) menyediakan penyelesaian alternatif tanpa menghadapi isu kestabilan. RFM memerlukan model PV arus-rintangan (I-R) khas untuk beroperasi. Buat masa ini, interpolasi tegak bersegmen boleh laras (PLI) untuk model PV khas ini tidak tersedia untuk RFM PVE. Kertas ini mencadangkan model PV I-R PLI boleh laras (IRPLI) untuk PVE yang menggunakan strategi kawalan RFM. Prestasi model PV ini beserta dengan PVE RFM dibandingkan dengan model PV interpolasi voltan-arus (IVPLI) bersama dengan PVE DRM. Keluaran IRPLI serupa dengan IVPLI pada pelbagai radiasi. Diskrepan dalam ralat bagi kedua-dua model PV adalah maksimum 6% berbanding dengan model PV satu diod (SDM). IRPLI 3.2 kali lebih cepat berbanding SDM dan 1.07 kali lebih lambat berbanding IVPLI. IRPLI juga dapat diintegrasikan dengan betul dengan PVM RFM tanpa sebarang isu kestabilan.

Kata kunci: Model Fotovoltaik, interpolasi tegak bersegmen, regresi tegak, penukar buck, pengawal PI.

1.0 INTRODUCTION

A Photovoltaic (PV) emulator (PVE) is a power converter that produces similar voltage and current characteristics as a PV module. It is useful during the development of the PV generation system. The system consists of three main components; which are the control strategy, power converter, and PV model [1, 2].

There is various type of control strategy used for the PVE. The common control strategy is the direct referencing method (DRM). The DRM can either be voltage control [3, 4] or current control [5, 6], depending on the PV model and closed-loop controller used for the PVE. Although the DRM is fairly simple, it is difficult to retune the closed-loop controller. This is because the DRM control strategy is highly affected by the change in the load and irradiance. The DRM commonly becomes unstable at high load and irradiance for current control[7, 8]. While the voltage control DRM becomes unstable when the load and irradiance are low. When using a switch mode power supply (SMPS) in PVE, the output voltage and current produce ripple. This ripple is fed into the PV model in the PVE, which produce oscillating reference input. Common closed-loop controller is designed to have a constant reference input. However, due to the oscillating input reference, the properly tuned closed-loop controller unable to work properly, resulting in instability problem.

To avoid the instability problem faced by the DRM, the resistance feedback method (RFM) is introduced. As mention before, the voltage and current contain ripple. However, there is no ripple for the resistance. When the non-ripple resistance reading is fed into the PV model, the input reference produced in not oscillating. This allows the properly tuned closed-loop controller to work properly and avoid oscillating problem. This control strategy uses a non-standard PV model that has resistance as the input instead of voltage or current. This is the limitation of the RFM since a specialised PV model is needed for this purpose. The look-up table method is used for the RFM [9-11]. Although this method is simple, it requires a lot of memory to store the data. The method is also not flexible since it requires a different set of data if the irradiance changes.

The direct calculation method is also being implemented for the RFM. This means that the model is computed directly, which does not require memory and is flexible. These include the reverse triangle method [12], integral controller [13], and binary search method [14]. Although this method is able to compute the specialised PV model with resistive input, it requires high computational power. A PVE needs to have a fast computation time to work properly [15, 16]. If the computation burden is high, but the computational power is low, the computational time becomes long and the PVE is unable to work properly.

Piecewise linear interpolation (PLI) is one of the ways to reduce the computation burden in the PVE. The current-voltage (I-V) PV model is modified to become the current-voltage PLI (IVPLI) PV model and used in the PVE [17, 18]. Since the accuracy of the PLI is low, this approach is rarely used. However, if the computation capability of the PVE is low, the PLI is useful, especially if the accurate emulation is not a priority. Besides the accuracy problem, the irradiance cannot be changed for the PLI PV model.

The RFM has the advantage of stable output compared to the DRM. However, the RFM requires a modified current resistance (I-R) PV model, which is able to receive resistive input. Currently, there is still no current-resistance PLI (IRPLI) PV model available to be used in the RFM for the PVE. There is also limited adjustment available for the PLI PV model used in the PVE.

This paper proposed an adjustable IRPLI PV model for the RFM PVE. It uses a buck converter and PI controller. The first contribution is the adjustable PLI PV model that uses linear regression to adjust the standard test condition (STC) voltages. The second contribution is the conversion of the IVPLI PV model to the IRPLI PV model for use in the RFM control strategy for the PVE. The proposed IRPLI RFM PVE is compared with the IVPLI DRM PVE as the benchmark.

2.0 METHODOLOGY

The proposed IRPLI PV model is used in the RFM PVE. The IRLPLI RFM PVE is then compared with the IVPLI DRM PVE. Both PVEs are displayed in Figure 1. For the DRM, the IVPLI PV model receives output voltage (V_o) and irradiance (G). The IVPLI PV model then calculates the PV current (I_{pv}), which becomes the reference current (I_{ref}). The comparison between I_{ref} and the output current (I_o) is conducted to ascertain the error (e). The proportional-integral (PI) controller utilizes the error (e) to calculate the suitable duty cycle (d) for the buck converter. The changes in d produce changes in V_o and I_o. The process is then repeated. For the RFM, the V_o is divided to I_o which mathematically calculates R_o. The Ro is fed into the IRPLI PV model as PV resistance (R_{pv}) to produce I_{ref}. The rest of the process is similar to the DRM.

Based on the parameters in Table 1, the IVPLI PV model is implemented based on Figure 2. The process starts by reading the V_{pv} and G. Then, the STC parameters are defined in the PV model. Based on the observation, the short circuit current (I_{sc}) and maximum power current (I_{mp}) are highly proportional to the G, the proposed adjustment of I_{sc} and I_{mp} are shown in Equation 1 and Equation 2, respectively. However, for the open circuit voltage (V_{oc}) and maximum power voltage (V_{mp}), the relationship is not linear to the G. However, the nonlinearity is not significant and linear regression still can be used for the STC adjustment. The proposed V_{oc} and V_{mp} adjustments are shown in Equation 3 and Equation 4, respectively.

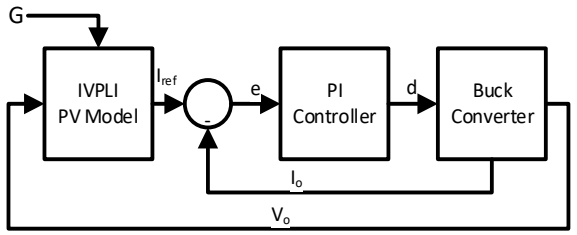

(a)

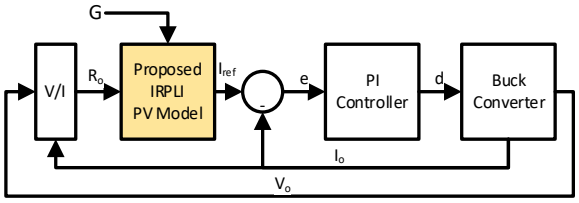

(b)

Figure 1 Control Strategy of PVE. a) DRM (using IVPLI PV Model). b) Resistance Feedback Method (using proposed IRPLI PV Model)

Table 1 STC parameters of the HHGJ100P(36) Solar Module

Parameters	Value
Open Circuit Voltage, V_{oc}	22.5 V
Short Circuit Current, I_{sc}	6.23 A
Maximum Power Voltage, V_{mp}	17.8 v
Maximum Power Current, I_{mp}	5.62 A

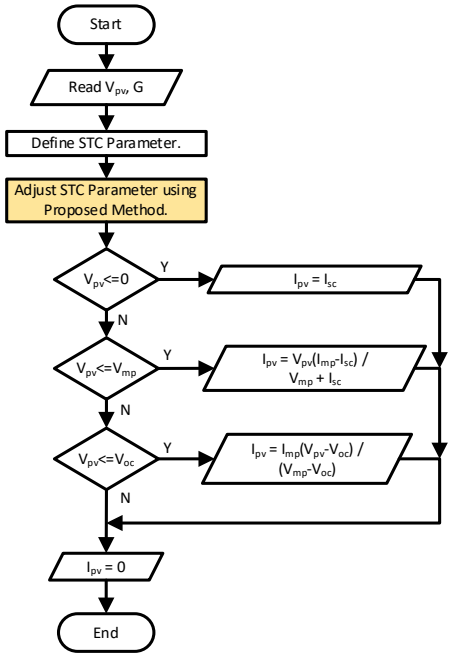

Figure 2 Flowchart of the IVPLI PV Model with proposed STC parameter adjuster

$$I_{sc} = \frac{G}{1000} * I_{sc(stc)} \quad \textbf{(1)}$$

$$I_{mp} = \frac{G}{1000} * I_{mp(stc)} \quad \textbf{(2)}$$

$$V_{oc} = m_{voc}G + c_{voc} \quad \textbf{(3)}$$

$$V_{mp} = m_{vmp}G + c_{vmp} \quad \textbf{(4)}$$

After the STC adjustment, the detection of segments based on the V_{pv} started. If Vpv is less than 0, the Ipv is equal to I_{sc}. If the V_{pv} is between 0 to V_{mp}, the I_{pv} follows Equation 5. If the V_{pv} is between V_{mp} and V_{oc}, the Ipv follows Equation 6. Both equations are based on the PLI approach with 2 segments.

$$I_{pv} = \frac{(I_{mp}-I_{sc})}{V_{mp}} V_{pv} + I_{sc} \quad for\ 0 \le V_{pv} \le V_{mp} \quad \textbf{(5)}$$

$$I_{pv} = \frac{I_{mp}(V_{pv}-V_{oc})}{V_{mp}-V_{oc}} \quad for\ V_{mp} < V_{pv} \le V_{oc} \quad \textbf{(6)}$$

The proposed IRPLI PV model for the RFM PVE is shown in Figure 3. The process starts by reading the R_{pv} and G. Then, the STC parameters are defined in the PV model. The proposed STC parameters adjuster is applied to determine the new STC parameters based on the G.

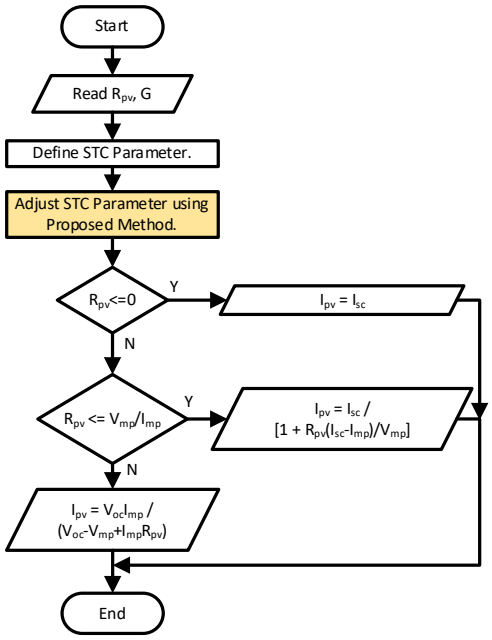

Figure 3 Flowchart of the Proposed IRPLI PV Model with STC parameters adjuster

The proposed IRPLI PV model used in the RFM PVE is derived from the IVPLI PV model. The V_{pv} in the IVPLI PV model is replaced with Equation 7. Equation 7 is substituted into Equation 5 to become Equation 8. The IVPLI PV model uses V_{pv} to determine the segment range, which is the limit divided at the V_{mp}. For the IRPLI PV model, the R_{pv} is used to determine the segment. Therefore, V_{mp} cannot be used for the segment separation. Instead, the maximum power resistance (R_{mp}) is used, which is shown in Equation 9. Therefore, the range of segments for Equation 8 is between 0 to R_{mp}. The second segment range is when the R_{pv} is between R_{mp} and infinity. Equation 7 is substituted into Equation 6 to become Equation 10.

$$V_{pv} = I_{pv}R_{pv} \quad (7)$$

$$I_{pv} = \frac{I_{sc}}{1 + R_{pv}\frac{I_{sc} - I_{mp}}{V_{mp}}} \quad for\ 0 \le R_{pv} \le R_{mp} \quad (8)$$

$$R_{mp} = \frac{V_{mp}}{I_{mp}} \quad (9)$$

$$I_{pv} = \frac{V_{oc}I_{mp}}{V_{oc} - V_{mp} + I_{mp}R_{mp}} \quad for\ R_{mp} \le R_{pv} \le \infty \quad (10)$$

The PVEs require an independent buck converter with a PI controller. To ensure a fair comparison between IVPLI DRM PVE and IRPLI RFM PVE, both PVEs use the same parameters for the buck converter and PI controller. These parameters are shown in Table 2. The buck converter used in the simulation uses the non-ideal components, as shown in Figure 4. The buck converter is designed to operate in the continuous current mode for the load ranging from 1 Ω to 20 Ω [19]. The V_o ripple factor is set to have a maximum of 1% [20]. The PI controller is adjusted to have a fast transient response while having a maximum current overshoot of 5% for all the load ranges.

Table 2 Parameters of the Buck Converter

Parameter	Value
Input Voltage, V_i	30 V
Switching Frequency, F_s	30 kHz
Inductance, L	1.5 mH
L Internal Resistance, r_L	0.3 Ω
Capacitance, C	200 µF
C Internal Resistance, r_C	0.1 Ω
Proportional Gain, K_p	0.03
Integral Gain, k_i	80

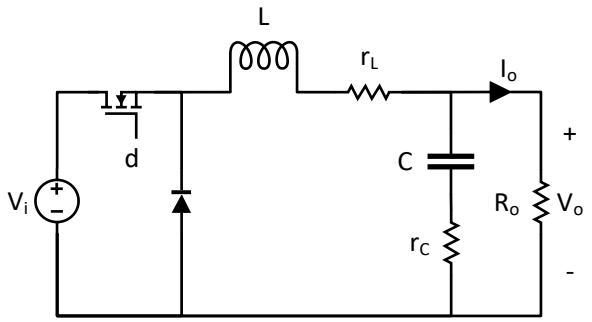

Figure 4 Circuit Diagram of Buck Converter

3.0 RESULTS AND DISCUSSION

A good PVE needs to be accurate. Therefore, the model needs to be close to the I-V characteristics of the PV module. Since the SDM PV model is widely used for modelling the PV module, this model becomes the reference for the accuracy test. Therefore, the IVPLI and proposed IRPLI PV models are compared with the SDM PV model. The I-V characteristic curves produced by the IVPLI, IRPLI, and SDM PV model are plotted in Figure 5 at various (250 W/m^2, 500 W/m^2, 750 W/m^2, and 1000 W/m^2).

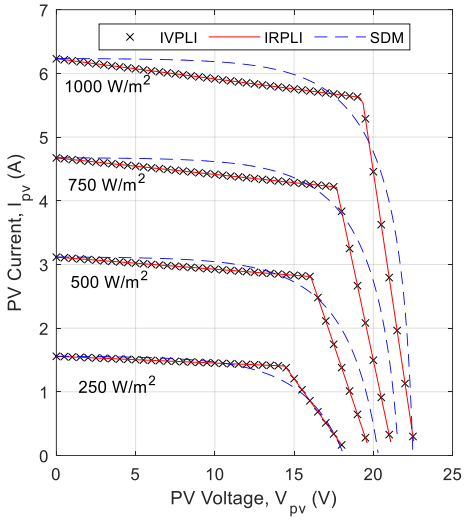

Figure 5 The I-V characteristic curves of the SDM, IVPLI, and proposed IRLPI at various G

The results show that the IVPLI and IRPLI have similar outputs. This is because the IRPLI is derived from the IRPLI PV model. Therefore, the output should be the same. However, both PLI PV models are different from the SDM. This is because it is based on different concepts. The SDM uses the Kirchhoff Current Law to derive the equation of the PV model. However, the IVPLI and IRPLI are based on the I-V characteristic curves of the PV module. Therefore, the results should be different.

The second analysis that can be observed from Figure 5 is the effectiveness of the proposed STC adjuster. When the G changes, the I_{sc} is able to change accurately, as shown in the y-intercept of the plot. For the Voc, which is located at the x-intercept of the plot, the proposed Voc adjustment using linear regression is not too accurate. This is because the relationship between V_{oc} and G is not linear. A higher level of regression is needed to obtain a more accurate V_{oc} adjustment. However, this leads to a higher computation burden, which needs to be avoided in the PVE application. The V_{mp} and I_{mp} point produced is not accurate. Both IVPLI and IRPLI PV models are inaccurate at this point. This is because only 2 segments of linear regression are used for this PV model. To improve this, an additional segment needs to be added. Nonetheless, adding segments increases the complexity of the PV model and increases the computation time.

To quantify the accuracy of the model, the current error (e_i) is used for the IVPLI and IRPLI PV models. The error is calculated using Equation 11. The PV models are simulated at various R_{pv} and G. The results of the simulation are displayed in Figure 6.

$$e_i = \frac{\left|I_{pv(sdm)} - I_{pv(pli)}\right|}{I_{pv(pli)}} \times 100\% \quad (11)$$

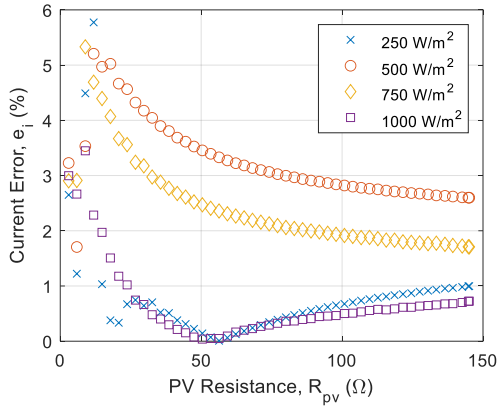

Figure 6 The e_i against R_{pv} of the IVPLI and proposed IRLPI compared to SDM

Since the IRLPI is derived from the IVPLI, both PV models produce same error. The results show that the highest error occurs around 4 Ω to 10 Ω of R_{pv}. This is the region where the constant current region and constant voltage region meet, also known as the maximum power point region. Since the IVPLI and IRPLI PV models are based on 2 segments of linear regression, the accuracy at the maximum power point region is low. As a result, the e_i is up to 6% for this region. Another noticeable observation is the error for the 1000 W/m2 is lower compared to other G results. This is due to the use of STC to model the PV models.

Since the PVE needs to operate in real-time, the computational burden needs to be considered to avoid any control failure. This is achieved by balancing the accuracy and the computation capability. If the computation capability is low, the simplified PV model, which commonly has low accuracy or limited operation is used. Therefore, the computation time (t_{com}) IVPLI, proposed IRPLI PV, and SDM PV models are tested using the 'Tic Toc' function in MATLAB. Each PV model is run 23,000 times to obtain the average t_{com}. The results are plotted in Figure 7.

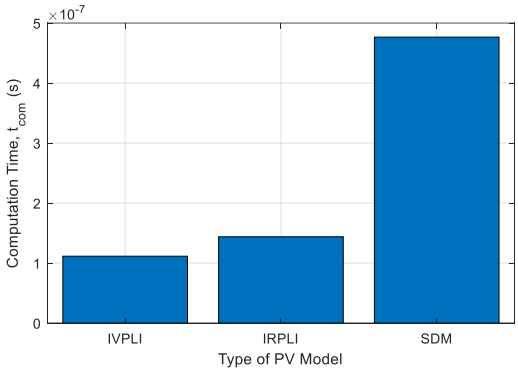

Figure 7 The t_{com} of SDM, IVPLI, and proposed IRLPI

The results show that the t_{com} for the IVPLI, proposed IRPLI, and SDM PV models are 109 ns, 139 ns, and 438 ns, respectively. Based on these results, the IVPLI and IRPLI PV models are, respectively, 4.0 and 3.2 times faster compared to the SDM PV model. This is significant since this approach is good if the computational power available in the PVE is low. The proposed IRPLI is slightly slower (1.07 times) compared to the IVPLI. This is due to a slightly complicated IRPLI PV model when compared to the IVPLI PV model.

The PVE that uses DRM commonly becomes unstable when the R_{pv} and G are high. As a result, the PI controller needs to be returned, which is not convenient, especially in the PVE application. This is because the DRM uses the PI controller to determine the operating point of the PVE. However, the RFM uses computation calculation to determine the operating point of the PVE, which prevents the PI controller from affecting the calculation of the operating point of the PVE. To show the effects, the PI controller for the closed-loop buck converter is tuned optimally to produce a fast transient response without the high overshoot, as shown in Figure 8. Note that at 0.2 s, the capacitor at the output still maintains the same voltage even after the load suddenly changes from 5 Ω to 2 Ω. As a result, a high spike of current cannot be avoided.

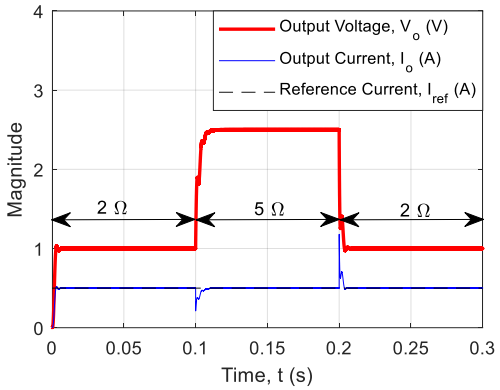

Figure 8 The V_o and I_o of the closed-loop buck converter with I_{ref} of 0.5 A during step-change of R_o between 2 Ω and 5 Ω

The closed-loop buck converter is then modified to the PVE using the DRM and RFM, independently. The DRM PVE uses the IVPLI PV model. While the RFM PVE uses the proposed IRPLI PV model. The G is set to 1000 W/m2 and the R_o is step-changed between 2 Ω and 5 Ω for every 0.1 s. This R_o values is chosen to test the performance of the PVE at constant current region (CCR) and constant voltage region (CVR). The divider of these regions is the maximum power point, which is 17.8 V and 5.02 A. Using Ohm's Law, the For the DRM, the V_o is measured and fed maximum power point resistance is 3.2 Ω. Therefore, 2 Ω and 5 Ω is a proper value to test the PVE at both region. The V_o and I_o are displayed in Figure 9.

The results shows that both DRM and RFM able to work properly with similar transient response when the R_o is 2 Ω. When the R_o changes to 5 Ω, the DRM produces oscillating V_o and I_o, while the RFM that uses the proposed IRPLI able to maintain a stable operation. Since the closed-loop buck converter able

to work properly when the R_o is 5 Ω, the instability is not cause by the not optimize tuning of the PI controller. This is aligned with research that compares DRM and RFM.

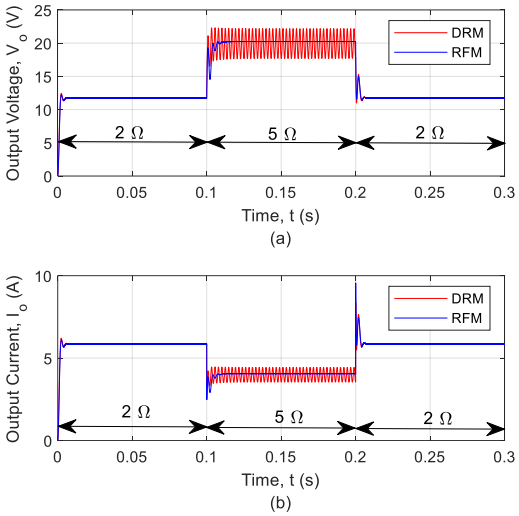

Figure 9 The a) Vo and b) Io of the PVE with G of 1000 W/m2 during step-change of Ro between 2 Ω and 5 Ω

The unstable operation of the DRM at high G is also observed in Figure 10. When the G is low and the R_o is set to 5 Ω, Both DRM and RFM are able to maintain their stability. Nonetheless, the DRM becomes unstable when G is high. While the RFM maintain a stable operation.

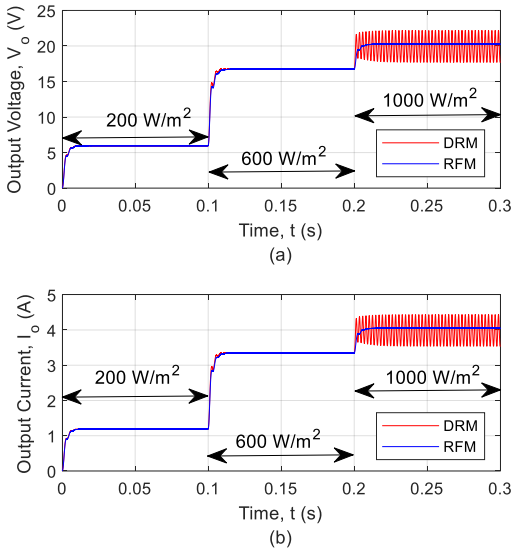

Figure 10 The a) V_o and b) I_o of the PVE with R_o of 5 Ω during step-change of G

For the DRM, the V_o is measured and fed into the IVPLI PV model. Since the V_o have ripple, the input to the IVPLI PV model is oscillated. In CCR, the I-V characteristic curve is near parallel to the x-axis. Any oscillation in the V_o at x-axis does not significantly change the I_{ref} at y-axis. However, in CVR, the I-V characteristic curve is near parallel to the y-axis. Any oscillation in the V_o at x-axis significantly change the I_{ref} at y-axis. This effect is illustrated in Figure 11. For the RFM, by using R_o, the oscillation of the V_o and I_o is eliminated. Therefore, input to the IRPLI is kept constant, thus producing a fixed I_{ref}, As shown in Figure 12.

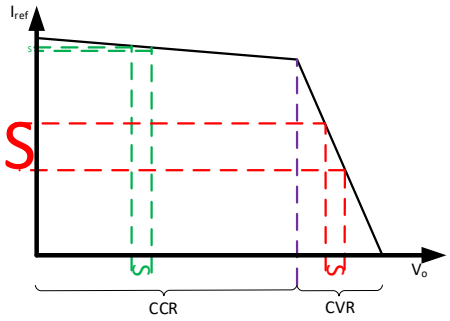

Figure 11 The effect of V_o oscillation on I_{ref} for DRM IVPLI PVE

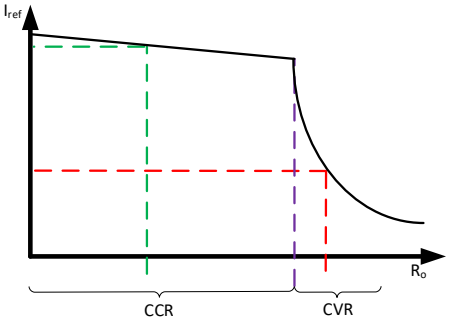

Figure 12 The effect of non-oscillating R_o input on I_{ref} for RFM IRPLI PVE

4.0 CONCLUSION

The proposed IRPLI PV model is a new way to design a PVE using the RCM control strategy. Based on the comparison with the IVPLI PV model, the accuracy is similar since the IRPLI PV model is derived from the IVPLI PV model. When the IRPLI PV model is compared with the SDM PV model, the accuracy of the PLI PV model is low, which is expected for this PV model. The error is less than 6% for the IRPLI PV model when compared to the SDM PV model. The advantage of the IRPLI PV model compared to the SDM PV model is the 3.2 faster computation time. This is suitable for the PVE with low computation capability and the accuracy is not the main concern. When the IRPLI PV model is implemented into the PVE using the RFM control strategy, the performance is good compared to the DRM PVE. There is no oscillation problem occurring at high load and irradiance. In conclusion, the IRPLI PV model performs well if the computation capability for the PVE is low and the accuracy of the PVE is not a major concern.

Acknowledgement

This research was supported by Ministry of Higher Education (MOHE) through Fundamental Research Grant Scheme (FRGS/1/2021/TK0/UTM/02/19). The authors would like to express gratitude to Universiti Teknologi Malaysia (UTM) for providing comprehensive facilities. Lastly, thanks to colleagues who have either directly or indirectly contributed to the completion of this work.

Conflicts of Interest

The author(s) declare(s) that there is no conflict of interest regarding the publication of this paper.

References

[1] M. Shahabuddin, A. Riyaz, M. Asim, M. M. Shadab, A. Sarwar, and A. Anees. 2018. Performance based Analysis of Solar PV Emulators: A Review. *2018 International Conference on Computational and Characterization Techniques in Engineering & Sciences (CCTES)*. 94-99.

[2] J. P. Ram, H. Manghani, D. S. Pillai, T. S. Babu, M. Miyatake, and N. Rajasekar. 2018. Analysis on Solar PV Emulators: A Review. *Renewable and Sustainable Energy Reviews*. 81(Part 1): 149-160.

[3] D. Subhi and R. Thabit. 2020. A New Low Cost Solar Array Emulator Based on Fuzzy and 32-Bit Microcontroller. *International Journal of Science and Engineering Investigations*. 9.

[4] D. Joshi and S. Sharma. 2019. PV Emulator Modeling and Design using Buck Converter. Applications of Computing. *Automation and Wireless Systems in Electrical Engineering*. 639-648.

[5] S. Esfandiari, S. H. Montazeri, and J. Milimonfared. 2020. Improvement of a High-accuracy Photovoltaic Emulator by Considering Wind Effect. *2020 11th Power Electronics, Drive Systems, and Technologies Conference (PEDSTC)*. 1-6.

[6] V. F. d. Souza, E. E. Behr, G. Waltrich, D. C. Martins, and R. F. Coelho. 2019. Photovoltaic Array Emulator Based on the Buck Converter. *2019 IEEE 10th International Symposium on Power Electronics for Distributed Generation Systems (PEDG)*. 843-848.

[7] U. K. Shinde, S. G. Kadwane, R. K. Keshri, and S. Gawande. 2017. Dual Mode Controller-Based Solar Photovoltaic Simulator for True PV Characteristics. *Canadian Journal of Electrical and Computer Engineering*. 40: 237-245.

[8] S. Jin, D. Zhang, and C. Wang. 2017. UI-RI Hybrid Lookup Table Method with High Linearity and High-Speed Convergence Performance for FPGA-based Space Solar Array Simulator. *IEEE Transactions on Power Electronics*.

[9] M. Farahani, M. A. Shamsi-nejad, and H. R. Najafi. 2020. Design and Construction of a Digital Solar Array Simulator with Fast Dynamics and High Performance. *Solar Energy*. 196: 319-326.

[10] P. Garg, Priyanshi, and G. Bhuvaneswari. 2018. Power Electronic Circuit based Implementation of a Solar PV Emulator using a Power Factor Corrected Buck Converter. *2018 IEEMA Engineer Infinite Conference (eTechNxT)*. 1-6.

[11] P. H. To and D. Q. Phan. 2017. A Photovoltaic Emulator using dSPACE Controller with Simple Control Method and Fast Response Time. *2017 International Conference on System Science and Engineering (ICSSE)*. 718-723.

[12] R. Ayop, C. W. Tan, and K. Y. Lau. 2019. Computation of Current-resistance Photovoltaic Model using Reverse Triangular Number for Photovoltaic Emulator Application. *Indonesian Journal of Electrical Engineering and Informatics (IJEEI)*. 7: 314-322.

[13] R. Ayop, C. W. Tan, and C. S. Lim. 2018. The Resistance Comparison Method using Integral Controller for Photovoltaic Emulator. *International Journal of Power Electronics and Drive Systems (IJPEDS)*. 9.

[14] R. Ayop and C. W. Tan. 2019. Rapid Prototyping of Photovoltaic Emulator Using Buck Converter Based on Fast Convergence Resistance Feedback Method. *IEEE Transactions on Power Electronics*. 34: 8715-8723.

[15] S. Raizada and V. Verma. 2016. Sizing Sampling Rate of the Integrated PV Simulator. *Industrial Electronics and Applications Conference (IEACon), 2016 IEEE*. 97-103.

[16] E. A. Mizrah, S. B. Tkachev, D. N. Poymanov, and A. S. Fedchenko. 2016. Nonlinear Compensation of Solar Array Simulators with Dual Power Regulation. *IOP Conference Series: Materials Science and Engineering*. 155: 012012.

[17] S. Masashi, Y. Naoki, and I. Muneaki. 2012. Development of Photovoltaic Cell Emulator using the Small Scale Wind Turbine. *Electrical Machines and Systems (ICEMS), 2012 15th International Conference on*. 1-4.

[18] D. D. C. Lu and Q. N. Nguyen. 2012. A Photovoltaic Panel Emulator Using a Buck-boost DC/DC Converter and a Low Cost Micro-Controller. *Solar Energy*. 86: 1477-1484.

[19] D. W. Hart. 2011. *Power Electronics.* Valparaiso University, Indiana: Tata McGraw-Hill Education.

[20] Ö. Ö, Y. Duru, S. Zengin, and M. Boztepe. 2016. Design and Implementation of Programmable PV Simulator. *2016 International Symposium on Fundamentals of Electrical Engineering (ISFEE)*. 1-5.